Japanese Journal of Gastroenterology and Hepatology

Research Article ISSN 2435-1210 |Volume 6

Increased Expression of GNL3L is Associated with Aggressive Phenotypes in Colorectal Cancer

Tiao-Tiao Z[1], Chen L[1], Bin-Hui P[1], Zhi-Hua X[1], Sheng X[1], Jia-Min Z[2], Chao-Yi W[2], Fang-Yan W[2], ChangLong XU[1*], Ying-Peng H[3] and XiaoLong Z[4*]

[1]Department for the Treatment and Study of Digestive Diseases, The 2nd Affiliated Hospital & Yuying Children's Hospital of Wenzhou Medical University, Wenzhou, China

[2]School of Basic Medical Sciences, Wenzhou Medical University, Wenzhou, China

[3]Department of General Surgery, The 2nd Affiliated Hospital & Yuying Children's Hospital of Wenzhou Medical University, Wenzhou, China

[4]Department of Critical Care Medicine, The 2nd Affiliated Hospital & Yuying Children's Hospital of Wenzhou Medical University, Wenzhou, China

***Corresponding author:**

Changlong XU,
Chief physician, Department for the Treatment and Study of Digestive Diseases, The 2nd Affiliated Hospital & Yuying Children's Hospital of Wenzhou Medical University, Wenzhou 325027, Zhejiang Province, China, Tel:138-6884-9191,
E-mail: xchlong@163.com

Xiaolong Zhang, Chief physician, Department of Critical Care and Pain Medicine, The 2nd Affiliated Hospital & Yuying Children's Hospital of Wenzhou Medical University, Wenzhou 325027, Zhejiang Province, China, Tel:139-5775-0507,
E-mail: china.zxl307@126.com; 1326719648@qq.com

Received: 28 Jun 2021
Accepted: 13 Jul 2021
Published: 20 Jul 2021

Citation:

Xiao-Long Z. Increased Expression of GNL3L is Associated with Aggressive Phenotypes in Colorectal Cancer. Japanese J Gstro Hepato. 2021; V6(21): 1-11

Keywords:

Colorectal cancer; GNL3L; Public data; Proliferation; MAPK signaling pathway

&Author contributions:

Tiao-Tiao Zhang, Lu Chen, Bin-Hui Pan, Zhi-Hua Xu, Sheng Xu, Jia-Min Zhang, Chao-Yi Wang, Fang-Yan Wang, Chang-Long Xu, Ying-Peng Huang, Xiao-Long Zhang and these authors are contributed equally to this work.

1. Abstract

1.1. Background and Objective: Guanine nucleotide binding protein-like 3-like (GNL3L) plays critical roles in development and progression of several types of human cancers. However, the function and clinical significance of GNL3L in colorectal cancer (CRC) remain unclear. In this study, the effect of GNL3L in CRC and its underlying mechanism were investigated.

1.2. Methods: The expression level of GNL3L in CRC and its potential prognostic value were evaluated based on publicly available data and were further investigated by in vitro experiments using colorectal cancer cell line. Co-expression network and bioinformatics analyses were utilized to identify the potential functional pathways of GNL3L in CRC. Finally, Gene microarray were designed to assess the downstream signaling pathways affected by GNL3L depletion, and key factors were analyzed by RT-qPCR.

1.3. Results: GNL3L was overexpressed in CRC tissues compared with adjacent normal tissues based on analysis of data from The Cancer Genome Atlas (TCGA) and the Gene Expression Omnibus (GEO). Higher

(CCLE) and RT-qPCR data. The results of in vitro experiments and tumor formation in nude mice model of xenograft indicate that the knockdown of GNL3L significantly suppressed RKO cell proliferation. Co expression networks and functional enrichment analysis revealed that GNL3L may be involved in the development of CRC via the MAPK signaling pathway. Furthermore, down-regulation of GNL3L in RKO cells inhibited the expression of RAP1, RAF, and ERK1/2 in the ERK/MAPK signaling pathway.

1.4. Conclusion: Our findings showed that a high expression level of GNL3L may serve as a potential target for therapy for CRC patients. GNL3L promotes proliferation of CRC cells through the ERK/MAPK signaling pathway.

2. Introduction

Colorectal cancer (CRC) is the second most common cancer and the third leading cause of cancer death in the world [1]. In China, the morbidity and mortality of CRC ranks fourth of all cancers [2], and CRC incidence continues to increase yearly with changes in dietary composition and lifestyle.

For now, curative surgery remains the only effective treatment for CRC, and early detection of resectable CRC is critical for future prognosis. Approximately 35%-55% of patients with advanced stage CRC have poor prognosis and high fatality rate due to lung and liver metastasis [3, 4]. Overall, traditional treatments (surgery, radiotherapy, chemotherapy, and traditional Chinese medicine therapy) do not exhibit significant curative effect or improve prognosis. Therefore, there is a significant clinical need for novel therapeutic targets for CRC.

GNL3L is a novel GTP-binding nucleolar protein of 582 amino acids, and functions in pre-nucleolar rRNA processing and cell proliferation [5, 6]. GNL3L, as a nucleo-cytoplasmic shuttling protein, regulates the cell cycle by interacting with chromosome region maintenance 1 (CRM1) through its C-terminal domain in the breast cancer cell line, MCF-7 [7]. Thoompumkal *et al.* reported that GNL3L interacts with leucine zipper down-regulated in cancer-1 (LDOC1) and regulates proliferation and apoptosis of HEK293T cells through the NF-κB pathway during tumorigenesis [5].

However, relatively few studies have investigated the role of GNL3L in the progression of colon cancer, and the underlying mechanism remains poorly understood. Therefore, the goal of this study was to use data from public databases, CRC cell lines, and tumor xenografts to examine GNL3L expression, function, and mechanisms in CRC. Our results revealed that GNL3L may be an effective target for the treatment of CRC.

3. Materials and Methods

3.1. Detection of GNL3L mRNA expression levels in CRC

CRC data from GEO, TCGA, and CCLE databases were analyzed for GNL3L expression levels. The included data were from microarray and RNA sequencing experiments uploaded before November 2019. MeSH-terms and entry terms were used to expand the search parameters in the GEO database (https://www.ncbi.nlm.nih.gov/geo/), with search terms of 'cancer', 'tumor', 'carcinoma' or 'neoplasm', and 'colorectum' or 'colon and rectum'. 'Homo sapiens' was used to limit the search range. Data were downloaded for a total of 12 microarrays from three platforms including 551 samples of CRC and 244 samples of para-cancer tissues with GNL3L expression information (Table 1). The normalized expression and median expression values were obtained from multiple probes of GNL3L. The RMA algorithm was applied in the R environment to normalize and transform the raw GEO data to expression values (v3.5.3) [8]. The removal of batch effects across platforms was performed using the "sva" Bioconductor package of R [9]. GNL3L expression in single series datasets and single platform datasets were compared between cancer and para-carcinoma tissue. The GNL3L expression data from TCGA (https://www.cancer.gov/about-nci/organization/ccg/research/structural-genomics/tcga) provided normalized counts of gene-level transcription. Gene Expression Profiling Interactive Analysis (GEPIA) was used to retrieve GNL3L expression data of CRC tissues. In addition, GNL3L expression and copy number data for 57 cell lines were obtained from The Cancer Cell Line Encyclopedia (https://portals.broadinstitute.org/ccle).

Table 1: Selected datasets from the Gene Expression Omnibus

ID	Type	Country	Case	
			CRC	non-CRC
GSE103512	GPL13158	USA	57	12
GSE77955	GPL96	USA	45	13
GSE44861	GPL3921	USA	56	55
GSE113513	GPL15207	China	14	14
GSE81558	GPL15207	Spain	42	9
GSE100179	GPL17586	Hungary	40	20
GSE122183	GPL17586	China	15	10
GSE73360	GPL17586	Italy	53	31
GSE84984	GPL17586	Italy	9	6
CSE31737	GPL5175	USA	40	40
GSE77434	GPL5175	Saudi Arabia	20	21
GSE24551	GPL5175	Norway	160	13
CRC, colorectal cancer.				

3.2. Cell Lines and Cell Culture

Human colorectal cancer cell lines (RKO, LoVo, HCT116, and SW620) were purchased from the Shanghai Cell Bank, Chinese Academy of Sciences (Shanghai, China). All cell lines were cultured in RPMI-1640 medium containing 10% fetal bovine serum (FBS; Ausbian) in 5% CO_2 at 37°C.

3.3. RNA Interference Lentivirus Construction and Infection

The GNL3L interference target sequence (target sequence: AGGAGATTTCCAACTATTA) and the negative control sequence (scramble sequence: TTCTCCGAACGTGTCACGT) were cloned

into the GV115 vector to generate a GNL3L shRNA recombinant plasmid and a negative control shRNA recombinant plasmid, respectively. Virus packaging was performed as follows. The two recombinant plasmids (20 μg) were packed with pHelper 1.0 Vector (packaging plasmid, 15 μg) and pHelper 2.0 vector (envelope plasmid, 10 μg) and were cotransfected into 293T cells using transfection reagent (Shanghai Genechem Co., Ltd., Shanghai, China). After 48 h of transfection, we collected the culture medium, sequentially concentrated it via ultracentrifugation, and then harvested shGNL3L lentivirus (no. LVpGCSIL-004PSC46597-1) and shCtrl lentivirus (no. psc3741). In the presence of Enhanced Infection Solution (ENi.S), and polybrene (Shanghai GeneChem Co., Ltd.), RKO cells were infected with lentivirus at multiplicity of infection (MOI) of 10. Infected cells expressing GFP protein were observed by fluorescence microscopy (cat. no. IX71; Olympus, Tokyo, Japan) to determine the infection efficiency. Cells were collected to perform qRT-PCR analysis after lentivirus infection.

3.4. Reverse Transcription-Quantitative Polymerase Chain Reaction (RT-Qpcr)

TRIzol reagent (cat. no. 3101-100; Shanghai Pufei Biotechnology Co., Ltd., Shanghai, China) was used to isolate total RNA from cells and tissues. Next, cDNA was synthesized by reverse transcription using M-MLV reverse transcriptase (Promega) in a total volume of 10 μl and the purified RNA was stored at -20°C. SYBR Premix Ex Taq (Takara Biotechnology Co., Ltd.) was used to perform qPCR. The conditions for PCR were as follows: 95 ◦C for 30 secs, 40 cycles of 95 ◦C for 5 secs and 60 ◦C for 30 sec. GAPDH was selected as an internal control, and the relative expression levels were determined by the following equation: $2^{-\Delta\Delta Ct}$($\Delta Ct=\Delta Ct^{target}-\Delta Ct_{GAPDH}$). The following primers were used in this study: for GNL3L, forward primer: 5'-CCGCCCTAAGAGCAACAGTAT-3', reverse primer: 5'-CACCAACACCATCATCAGCAT-3', for GAPDH, forward primer: 5'-TGACTTCAACAGCGACACCCA-3', reverse primer: 5'-CACCCTGTTGCTGTAGCCAAA-3', for RAP1, forward primer: 5'-GCCACCCGGGAGTTTGA-3', reverse primer: 5'-GGGTGGATCATCATCACACATAGT-3', for RAF-1, forward primer: 5'-TTTCCTGGATCATGTTCCCCT-3', reverse primer: 5'-ACTTTGGTGCTACAGTGCTCA-3', for ERK, forward primer: 5'-CGGGGCATCTTCGAGATCG-3', reverse primer: 5'-CAGAACAACGCCGTTTCAGTT-3'.

3.5. Cell Proliferation Assay

Cell proliferation was measured using the MTT Cell Proliferation Assay (ATCC). For each treatment condition, cells infected by shGNL3L or shCtrl (1000 per well) were transferred into 96-well plates and then cultured at 37 °C for 24, 48, 72, 96, and 120 h after attachment. The infected cells were incubated with 20 μL of MTT (Genview) for 4 h at 37 °C. The supernatants were removed, and then 100 μL of dimethyl sulfoxide (DMSO; Shanghai Shiyi Chemical Reagent Co., Ltd.; cat. no. 130701) was added. The Optical Density (OD) was measured at 490 nm using a microplate reader (cat. no. M2009PR; Tecan infinite).

3.6. Cell Cycle Analysis

Cells of the shCtrl and shGNL3L groups were seeded in six-well culture plates and incubated in complete medium to 80% confluence at 37 °C. After centrifugation at 1300 rpm for 5 min, the supernatants were discarded. The harvested cells were fixed with 75% cold ethanol at 4 °C for at least 1 h, washed twice with D-Hanks, and then stained using cell staining solution that contained 2 mg/mL propidium iodide (PI), 10 mg/mL RNase A, and 1 x D-Hanks. The fluorescence of DNA-bound PI in cells was measured by flow cytometry (cat. no. Guava easyCyte HT; Millipore), and the percentages of cells with different cell cycle phenotypes were calculated.

3.7. Apoptosis Assays

To detect cell apoptosis, the Caspase-Glo® 3/7Assay Kit (Promega) was used according to the manufacturer's instructions. Briefly, cells were seeded in 96-well plates and cultured in a CO_2 incubator at 37 °C for 5 d. We prepared the Caspase-Glo reaction solution according to the manufacturer's instructions. After cell counting, the concentration of the cell suspensions was adjusted to 1×10^4 cells/well at room temperature, and target cells and negative control cells were separately added to a new 96-well plate at 100 μl per well. A cell-free group with only the medium (100 μl/well) was used as the blank control. Cells were mixed with the Caspase-Glo reaction solution (100 μl/well) at 300-500 rpm for 30 min, and then incubated for 1 h at room temperature. Analysis of signal intensity was performed by flow cytometry.

3.8. Tumor Xenograft Growth Assay in Vivo

A subcutaneous xenograft model was established to estimate the effect of GNL3L on tumor growth *in vivo*. Six BALB/c nude mice (males, 4-weeks-old) were purchased from Shanghai Laboratory Animal Center (Shanghai, China) and randomly divided into two groups (three mice per group). Experimental procedures in this study were performed according to our institutional guidelines for using laboratory animals and were approved by the Medical Experimental Animal Care Commission of Wenzhou Medical University. RKO cells infected with shGNL3L or vector control were subcutaneously injected into the bilateral flanks of the mice. The weight, length, and diameter of tumors were measured every other day after 14 d.

3.9. Biological Function Analysis

To investigate the biological function of GNL3L in CRC, we adopted the GEPIA and Coexpedia (http://www.coexpedia.org/) online tools to identify GNL3L-associated genes that may be involved in CRC development [10]. Then, Gene Ontology (GO) and Kyoto Encyclopedia of Genes and Genomes (KEGG) pathway enrichment analyses were assessed using the DAVID 6.8 bioinformatics resource (https://david.ncifcrf.gov/home.jsp).

3.10. Microarray Analysis

RKO cells were infected with shGNL3L and shCtrl lentiviral vectors and total RNA was isolated using Trizol reagent according to the manufacturer's protocol. The extracted RNA was examined by NanoDrop 2000 and Agilent Bioanalyzer 2100 to obtain acceptable RNA, whose A260/A280 is in the range of 1.7~1.2, RIN ≥ 7.0 and 28S/18S>0.7, and thereby approved to microarry experiment. Differential expression genes were detected by Affymatrix Genechip and then subjected to signaling pathway enrichment analysis. The IPA software was used to analyze the downstream signaling pathway affected by GNL3L depletion, especially those closely related to tumor initiation and progression. Afterwards, the expression of significant molecules in the downstream signaling pathway after GNL3L silencing was confirmed by RT-qPCR.

3.11. Statistical Analysis

Statistical analysis was performed using the SPSS 18.0 software. Student's t-test for a comparison between two groups. A value of P less than 0.05 was considered to be statistically significant.

4. Results

4.1. GNL3L was Overexpressed in CRC Tissues and Cell Lines

GNL3L was overexpressed in colon cancer tissues compared with corresponding normal tissues in the TCGA database (Figure 1A and B). Expression levels of GNL3L in various types of CRC cell lines were in accordance with those in CRC tissues based on CCLE data (Figure 1C). The copy number and mRNA expression levels of various CRC cell lines are shown in Supplement (Table1). For the 12 GEO microarrays, there was significantly increased GNL3L expression level in CRC tissues compared with that in adjacent tissues (GSE77955, GSE77434, GSE73360, GSE31737, GSE122183, GSE24551, GSE10079, GSE103512, GSE84984, GSE113513, and GSE44861) (Figure 1D), and this trend was also observed in the same batch effect-free platform. Additionally, we selected several cell lines from the CCLE website including RKO, LOVO, HCT116, and SW620 for testing the mRNA expression levels of GNL3L in four CRC cell lines by RT-qPCR (Figure 1E). These results were consistent with those of the bioinformatics analysis, as well as those of the aforementioned previous studies.

4.2. GNL3L Knockdown Inhibited Proliferation of CRC Cells in Vitro and Tumor Growth in Vivo

To further investigate the function of GNL3L in CRC cells, RKO cells were infected with a lentivirus that expressed shCtrl or shGNL3L vectors. Infection efficiency was determined by detecting GFP fluorescence. After 72 h of infection with shCtrl or shGNL3L, green fluorescence was detected in more than 80% of the cells, indicated the successful infection of RKO cells with lentivirus (Supplement Figure 1A). Next, the mRNA of GNL3L in genetically modified RKO cells *in vitro* were determined using RT-qPCR analysis of cell samples at 72 h post-infection. The results demonstrated markedly decreased expression levels of GNL3L in the RKO cells infected with shGNL3L (Figure 2A). MTT assays revealed that GNL3L knockdown inhibited the proliferation of CRC cells (Figure 2B and C). To further determine whether GNL3L mediated tumorigenesis *in vivo*, stable GNL3L knockdown RKO cells (shGNL3L) and control RKO cells (shCtrl) were subcutaneously injected into the flanks of 4-week-old male BALB/c nude mice. As shown in (Figure 2D and E), we found that xenograft tumors grown from shGNL3L RKO cells had smaller mean volumes and lighter tumor weight than those grown from control cells.

4.3. GNL3L Knockdown Increased Cell Apoptosis and Induced Cell Cycle G1 Arrest in CRC Cells

To evaluate the effect of GNL3L knockdown on CRC cells, we use Caspase 3/7Assay Kit to investigate cell apoptosis and cell cycle. The results revealed that silencing of GNL3L in RKO cells led to a significant increase in apoptotic rates compared with controls ($P<0.01$; (Figure 3A)). To investigate an effect on cell cycle, the cell cycle distributions of CRC cells in different groups were analyzed by flow cytometry. As illustrated in (Figure 3B and 3C), GNL3L-null RKO cells showed persistence of cells in G1 phase and a marked decrease in the proportions of cells in S phase and G2/M phase, indicating that GNL3L depletion induced cell cycle G1 arrest.

4.4. Analysis of GNL3L Biological Function Using Public Data

To identify the potential biological functions of GNL3L, we analyzed changes in gene expression related to GNL3L expression. GNL3L co-expression networks were constructed from GEO and TCGA data via Coexpedia and GEPIA, respectively (Figure 4A and B). GO and KEGG pathway enrichment analyses were applied to the identified co-expressed genes using DAVID tools. (Figure 4C and D). The KEGG pathway analysis showed that the most significant enriched pathways were related to the "Ribosome", "Ubiquitin mediated proteolysis", "Thyroid hormone signaling pathway", "Cell cycle" and "MAPK signaling pathway".

4.5. GNL3L Knockdown Inhibited the ERK/MAPK Signaling Pathways in CRC Cells

The above analysis of genes with expression patterns related to GNL3L expression revealed enrichment of genes in the MAPK signaling pathway. To further certify the mechanism through which GNL3L exerted its function in the tumorigenesis and development of CRC, Affymatrix Genechip was used to detect the differentially expressed genes after down-regulating the expression of GNL3L in CRC cells. IPA analysis exhibited ERK/MAPK signaling pathways to be the top altered pathways of in GNL3L-deletion group in CRC (Figure 5A). we next investigated the function of GNL3L in CRC by using RT-qPCR to measure the levels of key factors of the ERK/MAPK pathway following GNL3L knockdown. As shown in Figure 5B-D, knockdown of GNL3L resulted in decreased levels of RAP1, RAF and ERK1/2 mRNA (Supplement Table 1).

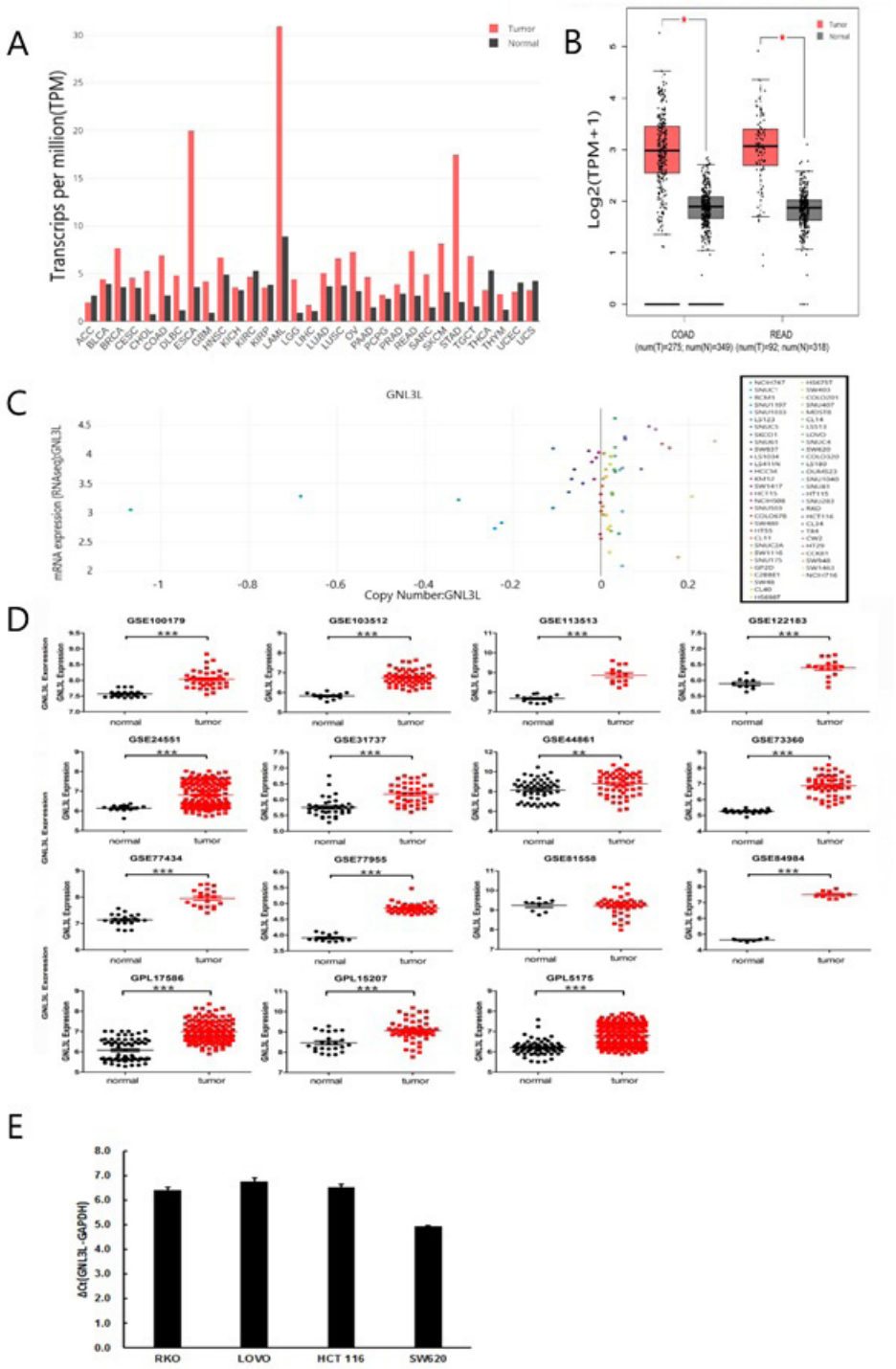

Figure 1: Overexpression of GNL3L in CRC tissues and cell lines. (A) The histograms indicate GNL3L expression levels in various types of cancer. (B) The expression of GNL3L was significantly higher in colorectal cancer tissues compared with normal tissues based on TCGA data (*P<0.001). (C) Scatter plot of GNL3L expression levels suggested that GNL3L is upregulated in different CRC cell lines (P=0.0219). Different colors denote different colorectal cancer cell lines. The scatter plot was downloaded from The Cancer Cell Line Encyclopedia. (D) GNL3L expression based on GEO microarray data. A total of 11 series showed that GNL3L was significantly overexpressed in colorectal cancer relative to normal tissues. After removal of batch effects, the platform microarrays were processed. GPL17586 contained GSE100179, GSE122183, GSE73360 and GSE84984; GPL15207 contained GSE113513 and GSE81558; GPL5175 contained GSE31737, GSE77434, and GSE24551 (*P<0.05; **P<0.05; ***P<0.001). Independent sample t-tests and paired t-tests were used for non-paired samples and paired samples, respectively. (E) mRNA levels of GNL3L in four CRC cell lines were detected by RT-qPCR. Note: ΔCt=ΔCttarget-ΔCtGAPDH. According to mRNA expression abundance: ΔCt ≤ 12, high target gene expression abundance; 12 <ΔCt <16, medium target gene expression abundance; ΔCt ≥ 16, low target gene expression abundance.

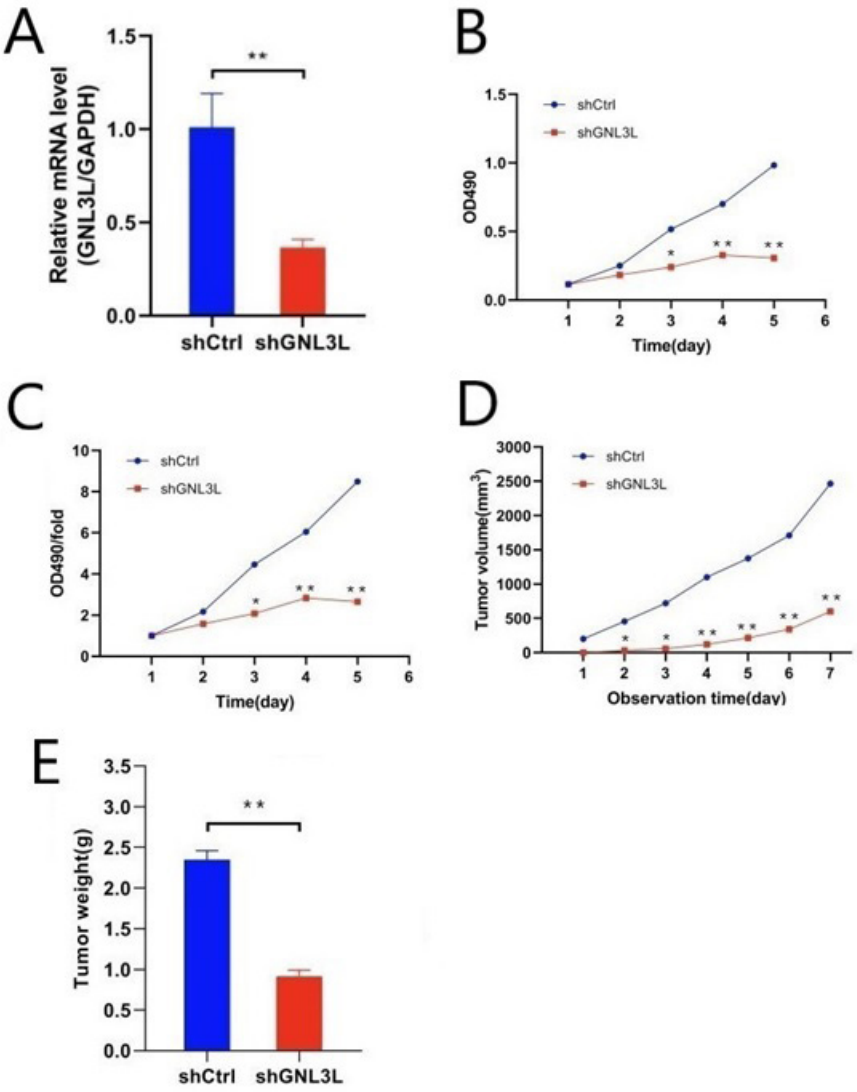

Figure 2: Knockdown of GNL3L efficiency and inhibited proliferation of RKO cells in vitro and tumor growth in vivo. (A) Detection of GNL3L knockdown efficiency in RKO cells by RT-qPCR that analysis of GNL3L expression in RKO cells following transfection with shGNL3L or shCtrl, as indicated. (B, C) MTT was used to assay proliferation and showed that GNL3L downregulation inhibited RKO cell proliferation. (D, E) Significant decreases in tumor volume and weight were observed in the GNL3L knockdown group. *P<0.05, **P<0.01 as compared to the shCtrl group.

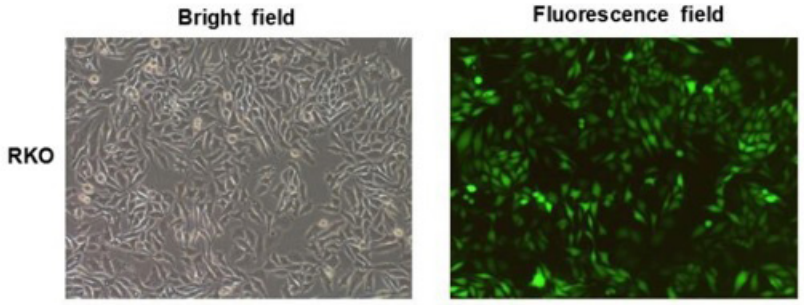

Supplement Figure 1: Bright-field (left) and fluorescent (right) images of RKO cells after infection with lentivirus containing GNL3L at magnification of ×100.

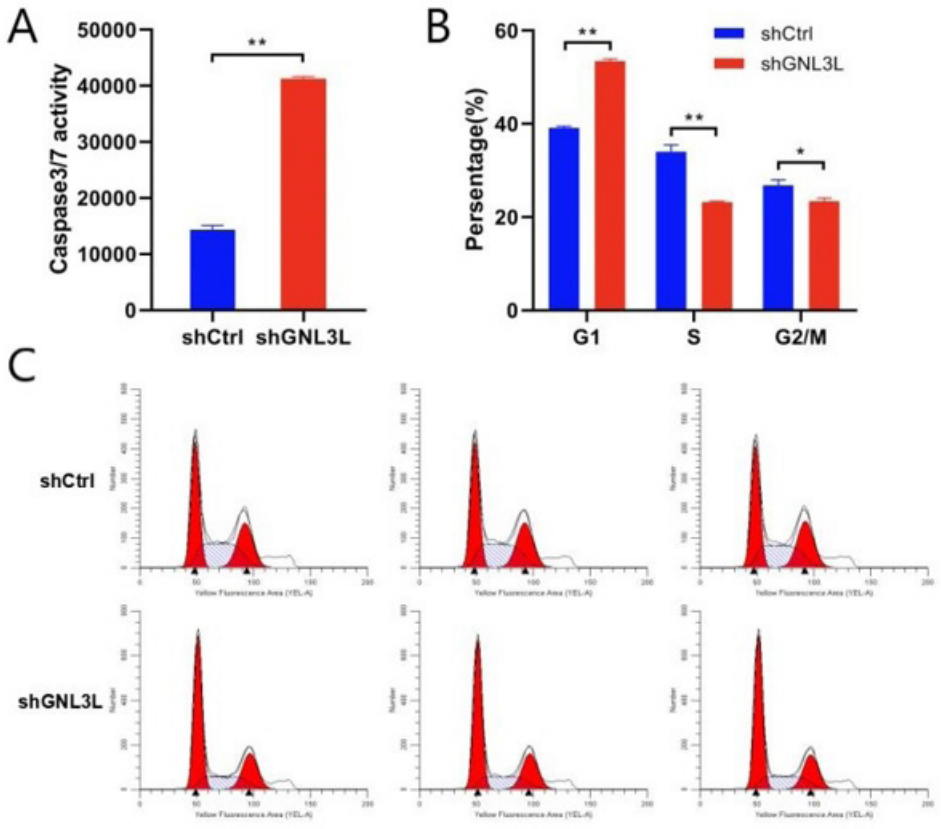

Figure 3: Knockdown of GNL3L induced apoptosis and G1 phase cell cycle arrest in RKO cells. (A) Caspase 3/7 activity was detected after knocking down GNL3L expression in RKO cells. (B, C) Cell cycle distribution was detected by flow cytometry in RKO cells infected with shGNL3L or shCtrl. *P<0.05, **P<0.01.

Supplement Table 1: The copy number and mRNA expression of different CRC cell lines

SW1116	0.0048	2.9650	SNU283	0.0490	3.7642
OUMS23	0.0411	2.6386	SNU503	-0.0008	3.1730
NCIH716	0.2590	4.2237	HS675T	0.0197	2.3203
SW480	0.0004	2.5541	HCC56	-0.0204	3.8669
SNUC2A	0.0042	3.1069	RCM1	-0.3236	3.2176
NCIH508	-0.0016	2.6288	RKO	0.0548	4.2952
LS123	-0.1089	3.0792	SNUC1	-0.6824	3.2807
SNU1197	-0.2413	2.7287	SW620	0.0321	4.6159
CW2	0.1247	4.4250	HCT116	0.0553	4.2579
SNU61	-0.0666	3.5765	LS411N	-0.0274	4.0562
HT115	0.0490	3.0218	LOVO	0.0307	3.7358
SNU1033	-0.2257	2.8252	LS1034	-0.0410	3.5007
SNUC5	-0.1085	4.1001	SW48	0.0121	3.6171
SNUC4	0.0320	3.9700	LS180	0.0327	3.6970
HCT15	-0.005	4.0308	SW403	0.0211	2.7677
SW1463	0.2067	3.2767	NCIH747	-1.0692	3.0488
CCK81	0.156	4.1050	SW1417	-0.0105	3.9414
COLO201	0.0213	3.8275	SW948	0.1757	2.2357
C2BBE1	0.0115	3.7396	HT290	0.1389	4.1758
LS513	0.0260	3.3099	KM12	-0.0153	3.5750
SW837	-0.0603	3.7395	T84	0.1094	4.4755
GP2D	0.0067	4.0123	CL14	0.0252	3.3364
HT55	0.0008	3.0243	CL40	0.0122	2.9558
MDST8	0.0231	2.6842	HS698T	0.0158	2.7171
SKCO1	-0.0729	3.3495	COLO678	-0.0001	3.3128
SNU81	0.0486	2.0877	COLO320	0.0325	4.1152
SNU1040	0.0430	3.7259	CL11	0.0029	3.4564
SNU175	0.0053	3.5805	CL34	0.0918	3.745934107
SNU407	0.0223	3.9630			

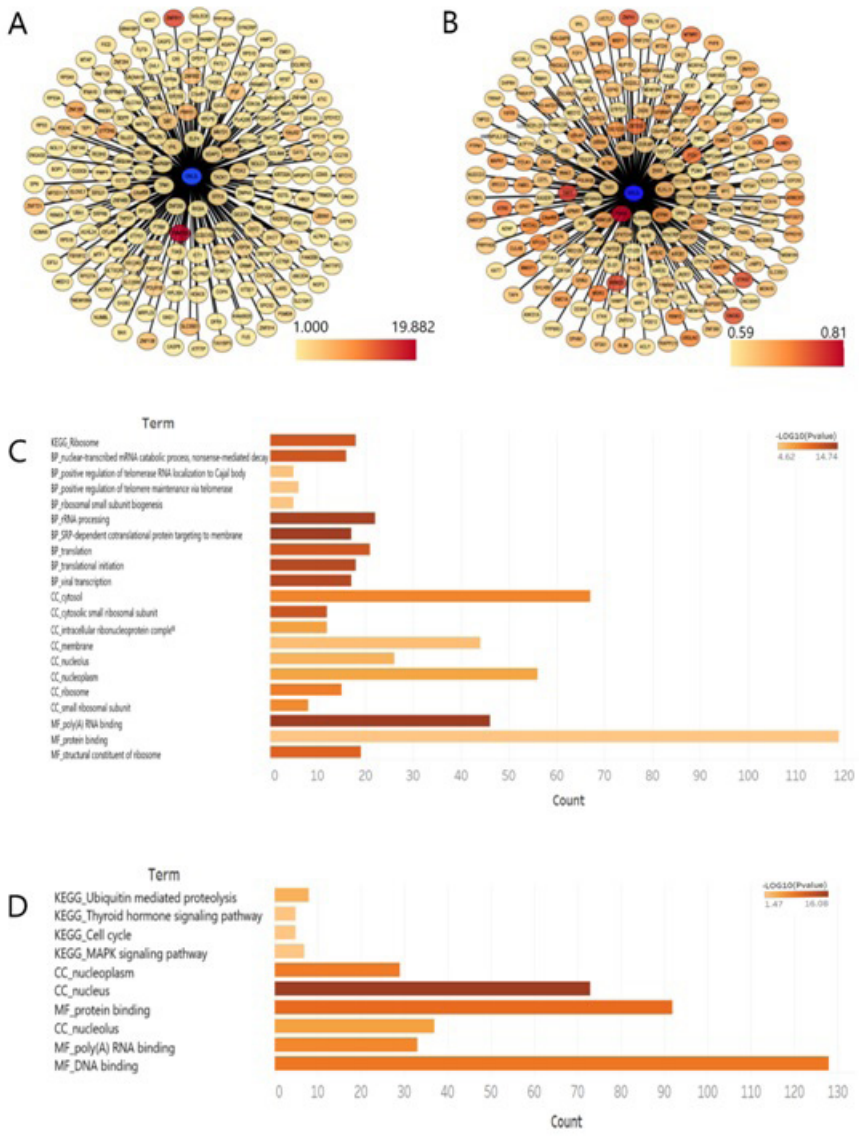

Figure 4: Biological function analysis of GNL3L in CRC. (A) Genes in the co-expression network of GNL3L were ranked based on scores from individual series dataset from GEO in Coexpedia. (B) Genes in the co-expression network of GNL3L were ranked by Pearson's correlation coefficient of TCGA data in GEPIA. (C) KEGG and Gene Ontology analysis of co-expressed genes associated with GNL3L, based on data obtained from the Coexpedia of GEO series dataset. (D) KEGG and Gene Ontology analysis of co-expressed genes associated with GNL3L, based on data obtained from the GEPIA of TCGA dataset. The horizontal axis represents the gene count for each functional term. Colors represent the P-value of function enrichment analysis, where light color indicates a lower correlation and dark color indicates a higher degree of association.

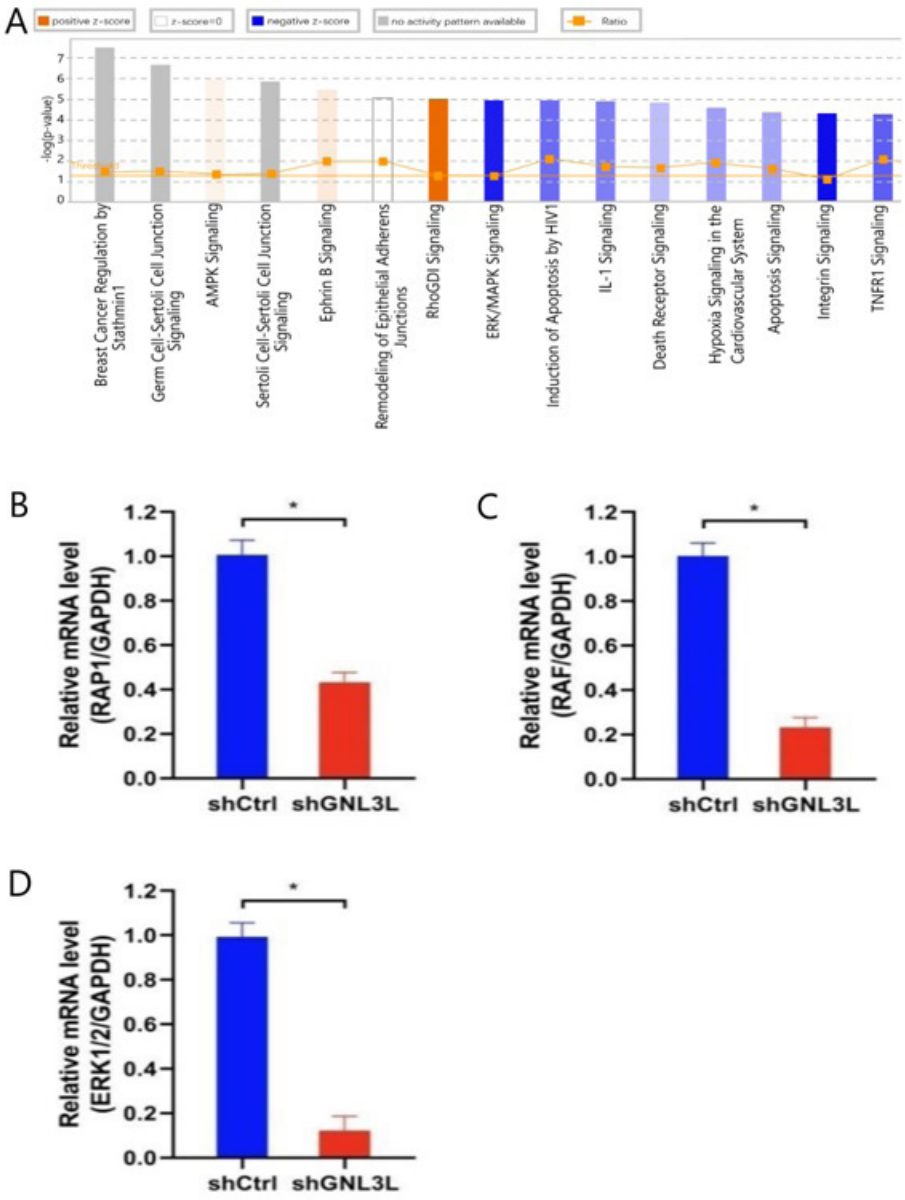

Figure 5: Knockdown of GNL3L inhibits the expression of RAP1, RAF, and ERK1/2 in the ERK/MAPK signaling pathway. (A) The enrichment of GNL3L in the classical signal pathways was shown that ERK/MAPK signaling pathway was inhibited by silence of GNL3L in RKO cells. The mRNA levels of RAP1 (B), RAF (C) and ERK1/2 (D) were detected by RT-qPCR after knockdown of GNL3L. The red color represents RKO cells transfected with shGNL3L, and black color represents cells transfected with shCtrl. *P<0.05 as compared to the shCtrl group.

5. Discussion

In recent years, gene-targeted therapy has been explored as a potential treatment for patients who suffer from advanced cancer. Oncogenesis and development of CRC are complex processes with multiple steps that can be affected by the imbalance between oncogenes and anti-oncogenes and changes in related signaling pathways. However, our understanding of CRC development and pathogenesis remains incomplete. Thus it is urgent to clarify the molecular mechanism of CRC to identify additional biomarkers for CRC-targeted therapy. GTP-binding proteins can hydrolyze nucleotide triphosphates to function as signal converters or molecular switches and participate in several key cellular events, including cell signaling, intracellular trafficking, proliferation, differentiation, and apoptosis [7, 11, 12]. Aberrant GTPase signaling has been observed in human diseases, including many different types of cancer. There is growing interest in determining the potential role of GTP-binding proteins in the development and progression of cancer.

GNL3L, a member of the GTP-binding protein family, shares high homology with nucleostemin (NS) and guanine nucleotide binding protein-like 2 (GNL2). Like NS, which is preferentially expressed in embryonic neural stem cells compared with differentiated progeny [13], GNL3L acts in cell growth and proliferation [14]. A recent analysis found that a significant fraction of various tumors expressed increased levels of GNL3L compared with paired normal tissues,

especially for colorectal, esophageal, and gastric tumors [15]. Our results were consistent with this analysis. Data from TCGA, GEO, and CCLE databases revealed significantly higher expression of GNL3L in CRC, and this altered expression was confirmed by measuring the levels of GNL3L mRNA via RT-Qpcr. GNL3L interacts with telomeric repeat binding factor 1 (TRF1) and promotes the metaphase-to-anaphase transition during mitosis [16,17], and GNL3L depletion destabilizes MDM2 and induces p53-dependent G2/M arrest [15]. GNL3L helps maintain tumorigenic property of tumor-initiating cells [18]. Interestingly, we found that knockdown of GNL3L in CRC cells significantly inhibited growth, decreased proliferation ability, and increased apoptosis-induced G1 phase arrest.

However, it is unclear how GNL3L promotes CRC, and determining the underlying mechanisms should be the focus of future work. We identified genes co-expressed with GNL3L and performed GO and KEGG enrichment analysis and found that GNL3L function may be related to the MAPK signaling pathway (P=0.03). The MAPK pathways relay intracellular signals and elicit physiological responses such as inflammatory responses and apoptosis in mammalian cells [19, 20]. Extracellular signal-regulated kinases (ERK) constitute a major subfamily of mitogen-activated protein kinases (MAPK), and these proteins act in the abnormal development of various tumors. The Ras/Raf/MEK/ERK pathway is the classical signal transduction pathway, with a three-stage enzymatic cascade reaction of MAPKs [21]. By switching Ras-family GTPases from the inactive GDP-bound form to the active GTP-bound form, external signals are transmitted from receptors on the cytoplasmic membrane to the interior of the cell. The biologically active GTP-Ras complex then activates Raf1, initiating a cascade involving MEK and then ERK activation [22-27]. Aberrant activation or dysregulation of the ERK/MAPK pathway easily results in uncontrolled cell proliferation and growth, giving rise to malignant transformation and cancer development. Activation of the Ras/Raf/MEK/ERK pathway helps induce the expression of vascular endothelial growth factor, which is involved in tumor invasion and metastasis of colorectal cancer [28]. Considering these properties, we hypothesize that overexpression of GNL3L can increase CRC cell proliferation and growth through the ERK/MAPK signaling pathway. To test this hypothesis, we performed Affymatrix Genechip and found that GNL3L knockdown suppressed the ERK/MAPK pathway remarkably. We detected expression of proteins in the ERK/MAPK signaling pathway in RKO cells with decreased expression of GNL3L.We observed significantly decreased expression of RAP1, RAF, and ERK1/2 via RT-qPCR. Based on our findings, GNL3L is a potential therapeutic target for treatment of CRC.

In summary, our results revealed overexpression of GNL3L in CRC and an effect of GNL3L to modulate cell proliferation through the ERK/MAPK signaling pathway. This is a novel mechanism of GNL3L-mediated oncogenic signaling in CRC progression and suggests GNL3L is a promising therapeutic target for patients with CRC.

6. Acknowledgement

This work was supported by the Zhejiang Provincial Medical and Health Science and Technology Project General Project (2019KY461), Wenzhou Science and Technology Bureau (Y20190060) and Zhejiang public welfare technology research plan/social development project (LGF20H070003).

References

1. Bray F, Ferlay J, Soerjomataram I, Siegel RL, Torre LA, Jemal A, et al. Global cancer statistics 2018: GLOBOCAN estimates of incidence and mortality worldwide for 36 cancers in 185 countries. CA Cancer J Clin. 2018; 68: 394-424.
2. Chen W, Zheng R, Baade PD, Zhang S, Zeng H, Bray F, et al. Cancer statistics in China, 2015. CA Cancer J Clin. 2016; 66: 115-32.
3. DeSantis CE, Lin CC, Mariotto AB, Siegel RL, Stein KD, Kramer JL, et al. Cancer treatment and survivorship statistics. 2014. CA Cancer J Clin. 2014; 64: 252-71.
4. Van Cutsem E, Nordlinger B, Adam R, Kohne CH, Pozzo C, Poston G, et al. European Colorectal Metastases Treatment Group. Towards a Pan-European consensus on the treatment of patients with colorectal liver metastases. Eur J Cancer. 2006; 42: 2212-21.
5. Thoompumkal IJ, Rehna K, Anbarasu K, Mahalingam S. Leucine Zipper Down-regulated in Cancer-1 (LDOC1) interacts with Guanine nucleotide binding protein-like 3-like (GNL3L) to modulate Nuclear Factor-kappa B (NF-κB) signaling during cell proliferation. Cell Cycle. 2016; 15: 3251-67.
6. Yasumoto H, Meng L, Lin T, Zhu Q, Tsai RY. GNL3L inhibits activity of estrogen-related receptor gamma by competing for coactivator binding. J Cell Sci. 2007; 120: 2532-43.
7. Thoompumkal IJ, Subba Rao MR, Kumaraswamy A, Krishnan R, Mahalingam S. GNL3L Is a Nucleo-Cytoplasmic Shuttling Protein: Role in Cell Cycle Regulation. PLoS One. 2015; 10: 0135845.
8. Gautier L, Cope L, Bolstad BM, Irizarry RA. Affy--analysis of Affymetrix GeneChip data at the probe level. Bioinformatics. 2004; 20: 307-15.
9. Leek JT, Johnson WE, Parker HS, Fertig EJ, Jaffe AE, Zhang Y, et al. sva: Surrogate variable analysis. R package version. 3.36.0, 2020.
10. Yang S, Kim CY, Hwang S, Kim E, Kim H, Shim H, et al. COEXPEDIA: exploring biomedical hypotheses via co-expressions associated with medical subject headings (MeSH). Nucleic Acids Res. 2017; 45: 389-96.
11. Bhuin T, Roy JK. Rab proteins: the key regulators of intracellular vesicle transport. Exp Cell Res. 2014; 328: 1-19.
12. Shimobayashi M, Hall MN. Making new contacts: the mTOR network in metabolism and signalling crosstalk. Nat Rev Mol Cell Biol. 2014; 15: 155-62.
13. Tsai RY, McKay RD. A nucleolar mechanism controlling cell proliferation in stem cells and cancer cells. Genes Devl 2002; 16: 2991-3003.
14. Du X, Rao MR, Chen XQ, Wu W, Mahalingam S, Balasundaram D. The homologous putative GTPases Grn1p from fission yeast and the

human GNL3L are required for growth and play a role in processing of nucleolar pre-rRNA. Mol Biol Cell. 2006; 17: 460-74.

15. Meng L, Hsu JK, Tsai RY. GNL3L depletion destabilizes MDM2 and induces p53-dependent G2/M arrest. Oncogene. 2011; 30: 1716-26.
16. Tsai RY. Nucleolar modulation of TRF1: a dynamic way to regulate telomere and cell cycle by nucleostemin and GNL3L. Cell Cycle. 2009; 8: 2912-6.
17. Zhu Q, Meng L, Hsu JK, Lin T, Teishima J, Tsai RY. GNL3L stabilizes the TRF1 complex and promotes mitotic transition. J Cell Biol. 2009; 185: 827-39.
18. Okamoto N, Yasukawa M, Nguyen C, Kasim V, Maida Y, Possemato R, et al. Maintenance of tumor initiating cells of defined genetic composition by nucleostemin. Proc Natl Acad Sci USA. 2011; 108: 20388-93.
19. Roux PP, Blenis J. ERK and p38 MAPK-activated protein kinases: a family of protein kinases with diverse biological functions. Microbiol Mol Biol Rev. 2004; 68: 320-44.
20. Zhang W, Liu HT. MAPK signal pathways in the regulation of cell proliferation in mammalian cells. Cell Res. 2002; 12: 9-18.
21. Cargnello M, Roux PP. Activation and function of the MAPKs and their substrates, the MAPK-activated protein kinases. Microbiol Mol Biol Rev. 2011; 75: 50-83.
22. Keshamouni VG, Mattingly RR, Reddy KB. Mechanism of 17-beta-estradiol-induced Erk1/2 activation in breast cancer cells. A role for HER2 AND PKC-delta. J Biol Chem. 2002; 277: 22558-65.
23. Sebolt-Leopold JS. Development of anticancer drugs targeting the MAP kinase pathway. Oncogene. 2000; 19: 6594-9.
24. Mahadev K, Wu X, Motoshima H, Goldstein BJ. Integration of multiple downstream signals determines the net effect of insulin on MAP kinase vs. PI 3'-kinase activation: potential role of insulin-stimulated H (2) O (2). Cell Signal. 2004; 16: 323-31.
25. Smalley KS. A pivotal role for ERK in the oncogenic behaviour of malignant melanoma? Int J Cancer. 2003; 104: 527-32.
26. Sato S, Fujita N, Tsuruo T. Involvement of 3-phosphoinositide-dependent protein kinase-1 in the MEK/MAPK signal transduction pathway. J Biol Chem. 2004; 279: 33759-67.
27. Santen RJ, Song RX, McPherson R, Kumar R, Adam L, Jeng MH, et al. The role of mitogen-activated protein (MAP) kinase in breast cancer. J Steroid Biochem Mol Biol. 2002; 80: 239-56.
28. Cassano A, Bagalà C, Battelli C, Schinzari G, Quirino M, Ratto C, et al. Expression of vascular endothelial growth factor, mitogen-activated protein kinase and p53 in human colorectal cancer. Anticancer Res. 2002; 22: 2179-84.